

A white super-stable source for the metrology of astronomical photometers

F. P. Wildi^{a*}, A. Deline^a, B. Chazelas^a

^a Observatory of Geneva, University of Geneva, 51 ch. des Maillettes, CH-1290 Sauverny

ABSTRACT

The testing of photometers and in particular the testing of high precision photometers for the detection of planetary transits requires a light source which photometric stability is to par or better than the goal stability of the photometer to be tested. In the frame of the CHEOPS mission, a comprehensive calibration bench has been developed. Aside from measuring the sensibility of the CHEOPS payload to the different environmental conditions, this bench will also be used to test the relative accuracy of the payload. A key element of this bench is an extremely stable light source that is used to create an artificial star which is then projected into the payload's telescope. We present here the development of this payload and the performance achieved.

Keywords: exoplanets, photometric transits, stable light source

1. INTRODUCTION

To test the stability of a photometer the simple solution is to use a light source which stability is better than the photometer to be tested. However, the regular lab sources have nowhere near the stability that is required for the current generation of photometers used for the detection and the characterization of planetary transits,

In the frame of the CHEOPS mission (see section 2), a comprehensive calibration bench has been developed. The core measurement that this bench is used for is the stability measurement of the reduced photometric signal. To be able to perform such a measurement, the bench relies on the very high stability of a light source used to generate an artificial reference star. This paper covers the development and characterization of this source

2. THE CHEOPS MISSION

The CHaracterising ExOPlanet Satellite (CHEOPS) is a joint ESA-Switzerland space mission dedicated to the characterization of exoplanet transits by means of high precision photometry [1]. Its launch is expected end of 2017. The CHEOPS instrument will be the first space telescope dedicated to search for transits on bright stars already known to host planets. By being able to point at nearly any location on the sky, it will provide the unique capability of determining accurate radii for a subset of those planets for which the mass has already been estimated from ground-based spectroscopic surveys. CHEOPS will also provide precision radii for new planets discovered by the next generation ground-based transits surveys (Neptune-size and smaller). The main science goals of the CHEOPS mission is to study the structure of exoplanets with radii typically ranging from 1 to 6 Earth radii orbiting bright stars. To reach its goals CHEOPS will measure photometric signals with a precision of 20 ppm in 6 hours of integration time for a 9th magnitude star. This corresponds to a signal to noise of 5 for a transit of an Earth-sized planet orbiting a solar-sized star (0.9 solar radii). This precision will be achieved by using a single frame-transfer backside illuminated CCD detector cooled to 233K (-40C) and stabilized within ~10 mK. The CHEOPS optical design is based on a Ritchey-Chretien style telescope with 300 mm effective aperture diameter, which provides a defocussed image of the target star while minimizing stray light using a field stop and baffle system. As CHEOPS will be in a LEO orbit, straylight suppression is a key point to allow the observation of faint stars. The telescope will be the only payload on a spacecraft platform providing pointing stability of < 8 arcsec rms. It represents a breakthrough opportunity in furthering our understanding of the formation and evolution of planetary systems.

Despite two highly successful space missions dedicated to transit searches (CoRoT and Kepler) and almost two decades of high-precision radial velocity measurement campaigns, the number of exoplanets in the mass range 1-30 M_{Earth} for which both mass and radius are to a good precision known, is extremely limited. This originates from the fact that these masses cannot be measured accurately enough by current Doppler methods for most of the CoRoT and Kepler targets. They are simply too faint to allow the required precision in radial velocity to be reached. The goal of CHEOPS is to

*francois.wildi@unige.ch

significantly increase the sample of objects for which both quantities are known. [1] describes the scientific objectives and challenges for the scientific community.

3. THE CHEOPS INSTRUMENT SYSTEM

The CHEOPS payload consists of only one instrument [2], a space telescope of 300mm clear aperture diameter, with a single focal plane. The instrument assembly, also called CHEOPS Instrument System (CIS, fig. 1) is composed of four main units:

- 1) The Baffle and Cover Assembly (BCA) minimizes the stray-light and includes a protective cover and release mechanism.
1. The Optical Telescope Assembly (OTA) includes the structure carrying the telescope, the Back End Optics (BEO), the Focal Plane Module (FPM), and the radiators. In order to minimize the impact of thermo-elastic deformations on the instrument pointing, the optical heads of the platform star trackers will be mounted on the OTA, in proximity of the isostatic mounts of the instrument.
- 2) The Sensor Electronics Module (SEM)
- 3) The Back End Electronics (BEE)

CIS main specifications are given in the table below:

Table 2. CHEOPS Instrument System (CIS) main specifications

Entrance pupil diameter	320mm
Central obstruction diameter	68mm
Working F/#	8.38 @ 750 nm
Telescope field of view diameter	0.32°
Spectral range	400 – 1100 nm
Pixel size / Plate scale	13 microns / 1 arcsec/pixel
Detector focal plane	1024x1024 pixels
Detector Temperature	233K
Detector temperature Stability	10mK
Instrument total Mass	<60kg including system margin
Instrument total nominal power	<60W orbit averaged including margin
Photometric stability	20 ppm over 6 hour transit

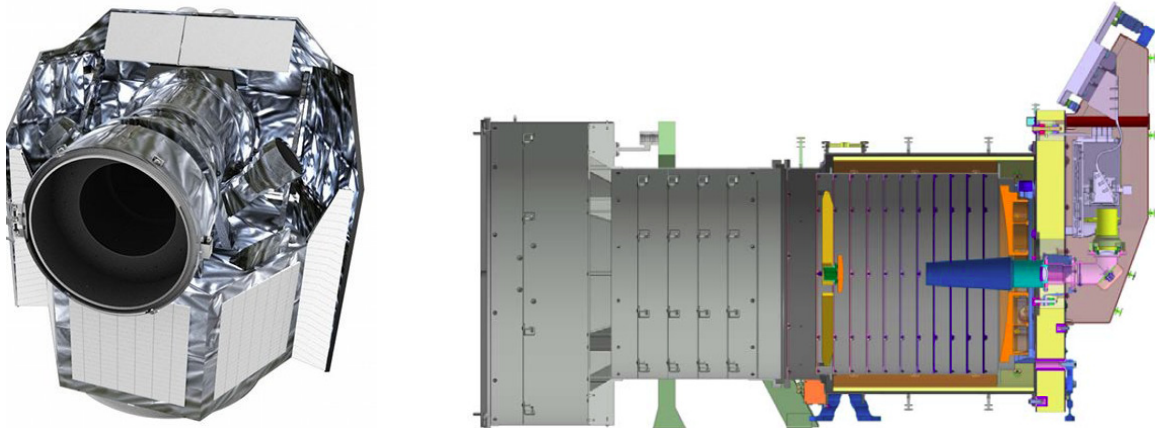


Figure 1. The CHEOPS satellite instrument L/h, and a cut through the CHEOPS instrument system R/h.

4. THE CHEOPS CALIBRATION BENCH

An important part of the CHEOPS performance budget hinges on our capability to correct the photometry for the effects of the environmental variations on the sensor. To this purpose an elaborate bench has been built to produce a geometrically and photometrically very stable beam that we can feed through an optical window into the CHEOPS telescope as it sits in the thermal vacuum chamber during the space environment tests. See ref [3]

This beam is oversized, collimated, and it can be steered to explore the full field. Its pupil is also steered so that we can compensate for differential position variations between the calibration bench and the payload in the vacuum chamber

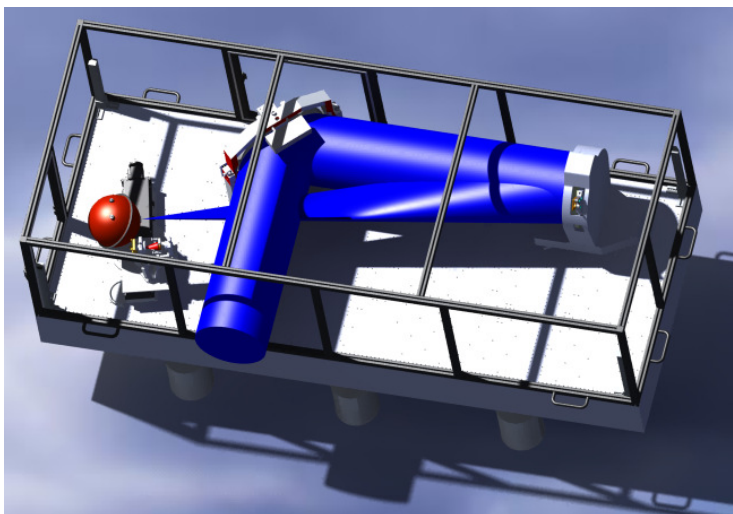


Figure 2. The CHEOPS calibration bench. After it exits the bench the beam goes through a window into the space environment simulator.

During the pre-flight validation campaign, the CHEOPS payload will be subjected to a number of different tests which primary purpose is to verify that the post-processed photometric signal has the high stability required by the mission. Part of the stability error of the payload + calibration bench system comes of course from the bench is self. The primary element that drives the stability of the bench is the light source used to produce an artificial star at the bench input focus. To guarantee that the photometric error is as small as possible we have developed in the frame of this project what we call a super-stable source (SSS).

5. THE SUPER STABLE SOURCE

Typically, for laboratory work in broadband light, quartz-tungsten halogen bulbs (QTH), Xe arc lamps are used. More recently, a very broad spectrum source called Laser Driven Light Source^{TM1} has become popular in the astronomical community (see spectrum below). The QTH lamps are notoriously "cold" for work in the visible wavelength range. This means that they lack the blue part of the spectrum and that their radiance is low. Xe arc lamps are bulky and can be somewhat unstable geometrically but produce a usable spectrum in the visible range

For CHEOPS, we have chosen to use an LDLS as primary source because its 10'000K color temperature offers both a flat spectrum across the visible and a high radiance that allows a sizable amount of power to be coupled even in a monomode fiber.

Any of the sources listed has typically a luminous power output variation of in the 1-3% p2v range, i.e. 10'000 to 30'000ppm over the 6 hours which is the duration over which the CHEOPS performance is specified. It is obvious that a lamp such as listed above cannot be used without having its flux stabilized. For this reason, the Observatory of Geneva has developed a luminous power control system that transforms the LDLS in what we call Super Stable Source. This system can also in principle be used to stabilize QTH and Xe arc lamps.

¹ from the Energetiq company

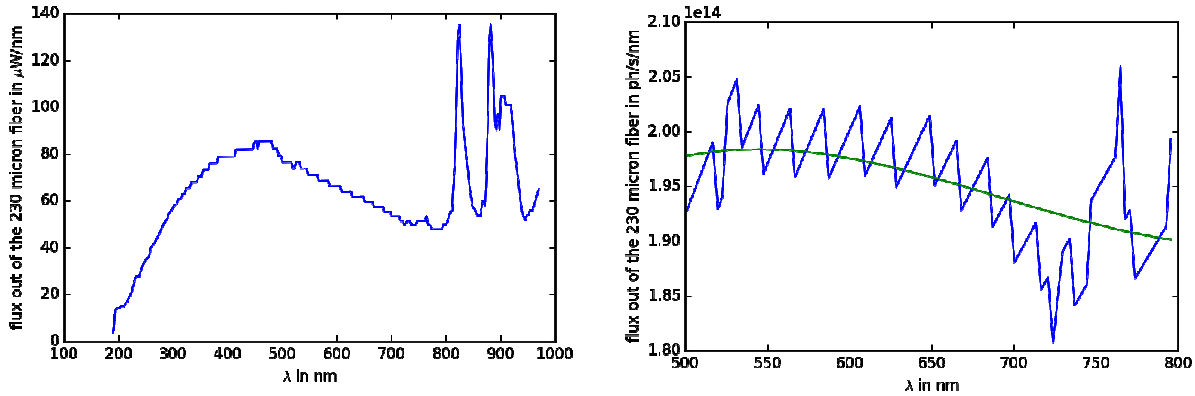


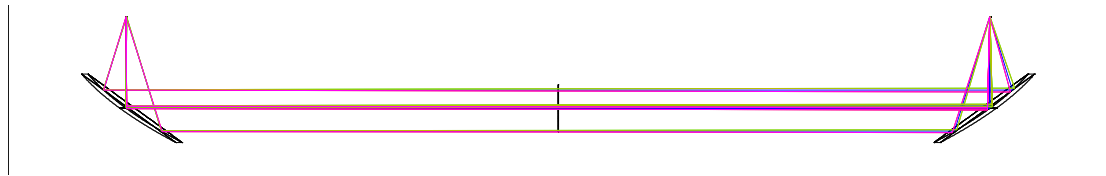
Figure 3. The power spectral density of the LDLS flux after 1 meter of 230 micron core fiber. L/h: Expressed in microwatt/nm over the spectral range covered by our measurement R/h expressed on ph/s/nm over the 500-800nm range

To allow it to work with different type of sources, it was decided to implement the power control as downstream modulation rather than trying to control primary source parameters like current in a QTH or ballast resistor current in an Xe arc lamp. Given its sophistication, it would be difficult to know with which parameter to play in the case of the LDLS.

One of the advantages of the LDLS is its high radiance. It allows to inject easily a substantial amount of light in a fiber. It was decided to keep the light in that format for the convenience. Therefore a system with a fibered input and a fiber output is called for. Between the two a system must be implemented to control the amount of light.

6. MODULATOR AND LIGHT CONTROL DESIGN

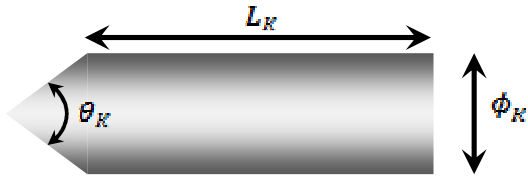
Our system features a collimator – decollimator arranged symmetrically. Between the two, a collimated beam lends itself to optical processing, in particular to power modulation. To make it as wide band as possible the system is fully catoptric, being made of a pair of off-axis parabolas.



The collimator decollimator is built with 2 off-axis parabolas from Newport, 1,5” in diameter and 2” in focal length. The mirrors are silver coated. The beam aperture out of the input fiber is 0.22, thus the beam size on the parabolas is approximately 22mm in diameter.

Given the size of the input size of the input fiber of 230 microns, and mechanical tolerances in the order of the 0.1mm (apart for the positioning of the output fiber that is ensured by a standard 3 axis translation stage with micron sensitivity), the transmission of the collimator decollimator for an output fiber should be around 75%. In addition there is the loss created by the knife, which adds up another 25% of loss.

The knife is a cylinder with a conical end towards the beam. The diameter and length of the cylinder and the aperture of the cone completely define the geometry.



The length of the knife depends on the travel of the positioner and the required part for mounting. In order to keep the fixing system off the beam, the part that crosses the beam must be longer than the travel of 20 mm. Allowing 30 mm the fixing system and margins, the length of the knife is set to 60 mm.

More arbitrarily, the angle and the diameter are chosen equal to 90° and 14 mm respectively. As the use of the knife is to balance the flux variations of the original light source, the chosen base flux has to be lower than the minimum flux of the source. Therefore, in practice, the knife will always be occulting a part of the collimated beam. Thus, the cone geometry is only used to limit high variations while approaching the center of the beam where the intensity is higher, and hence to increase the resolution. As for the diameter, it directly characterizes the attenuation in terms of resolution and amplitude. In first approximation, one can consider that the additional occulted part of the beam equals the step movement of the positioner times the diameter of the knife. In other words, when the linear stage moves forward, the occulting area increases by a rectangle ($L_{step} \times \phi_K$). Thus, even when occulting the brightest area of the beam, the resolution with a step of 1 nm would be better than 0.1 ppm. The maximum reachable attenuation is evaluated the same way, considering a maximum velocity of the stage of 4.5 mm/s and an occulted area with a low intensity. In this case, the best reachable value is 5% per second, which corresponds to 0.5 % per point at a sampling frequency of 10 Hz.

These values comply with the requirements even if they are the worst expected ones. As they are proportional to the knife diameter in first approximation, they won't be affected even by a typical surface roughness ($< 10 \mu\text{m}$).

The knife is fixed to the positioner via a mounting support. Screws ensure its fixation on the stage while the knife is blocked by a combination tube/pin, similar to the one used for the fibers.

7. THE FEEDBACK LOOP

The stabilization of the source flux is achieved with the opto-mechanical design described above. The feedback loop that controls the system is represented in the block diagram below. The source flux enters the SSS where the OAP mirrors ensure the fiber-to-free-space transition. The action of the feedback loop occurs at the level of the free space beam thanks to the attenuator. It is driven by the workstation that computes the value of the gain as a function of the current position of the attenuator.

On the diagram, the gain corresponds to the command that the workstation sends to the attenuator. This command is calculated dynamically due to the fact that the gain value depends on the current position of the attenuator. As shown on the following graphs, the attenuation does not vary linearly with the position of the attenuator in the free-space beam, which is due to the Gaussian power repartition in the beam and cone-shaped end of the attenuator. Therefore, the influence of a given increment in position does not have the same effect when the attenuator is in the middle or at the edge of the beam.

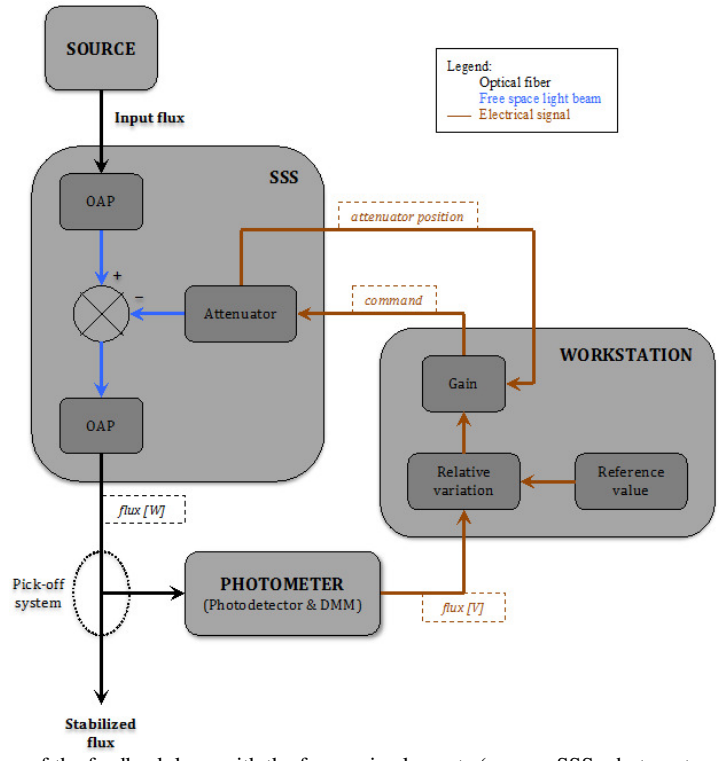


Figure 4. Block diagram of the feedback loop with the four main elements (source, SSS, photometer and workstation). In order to highlight the interactions between the SSS and the workstation, these two blocks have been detailed. The legend in the upper right corner shows the nature of the connections (fibers, free space beam or electrical cables). The pick-off system is not specified and can be any device as long as it gives a constant output/picked-off fluxes ratio.

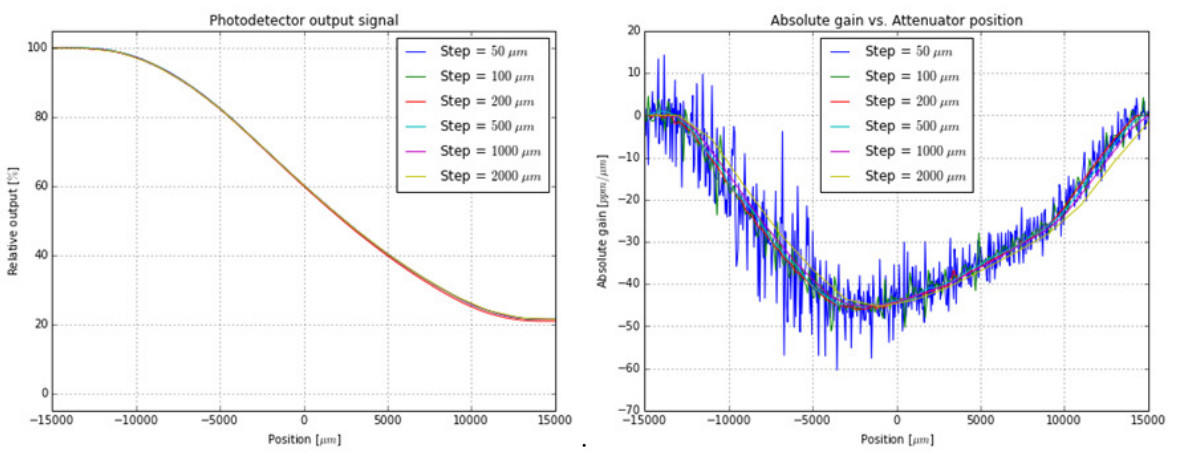


Figure 5. The SSS output flux for different position of the attenuator through a beam of 25mm (left). The attenuation per unit of distance (ppm/μm) measured on the left curves (equivalent to the derivatives) (right). The step values represent the spatial sampling period of the measurement.

The absolute gain (in ppm/μm) represents the attenuation relative to the zero attenuation value. However, a gain relative to the actual value of the flux is required as an input command for the attenuator. This relative gain is estimated with an optimal 7-degree polynomial fit, which is used as a reference for the dynamical gain calculation.

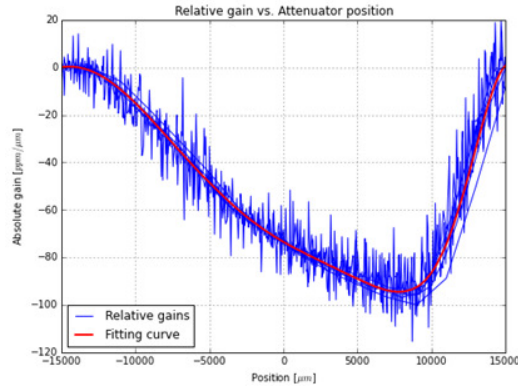


Figure 6. The relative attenuation per unit of distance achieved with the attenuator. The red curve is the optimal best-fit polynomial (degree 7) used to calculate the attenuation.

The feedback loop has two functioning modes.

The first mode, *slow* mode, sends a command to the attenuator and waits for it to reach required position before measuring another point with the photometer. In this case, the maximum sampling frequency of the system varies between 8 and 10 Hz.

The second mode, *continuous* mode, sends a command to the attenuator and directly measures another point with the photometer without waiting for the attenuator to be in place. In this case, the maximum sampling frequency of the system varies between 12.5 and 14 Hz, but the performances are degraded (see below).

8. OPTO-MECHANICAL DESIGN

We focused on keeping the system as simple as possible while keeping the nice broadband properties of our primary source. The beam path goes essentially from one large input fiber to an output fiber with the knife modulator in-between with only two reflective surfaces. While the input fiber is aligned statically, a motorized linear stage is mounted on a manual 3 axis platform at the output. The manual stage is used to align the fiber to the output focus of the focusing parabola and the motorized stage is used to switch between fibers when needed. One can for instance choose to mount 2 monomode fibers covering a different spectral range or mount on one side a large fiber to maximize throughput to feed a flat field source.

The complete light control system is packaged in a shoebox size housing, excluding the primary source and the reference sensor which need to be located as close to the point of use of the light as possible. The figures below show our opto-mechanical implementation:

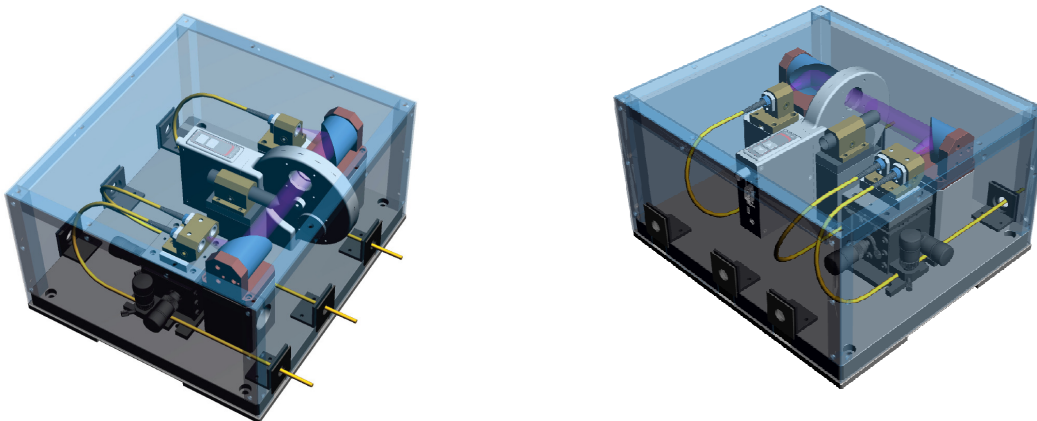


Figure 7. 3D renderings of the light control box, the keystone of the super stable source. Light enters the system on the top fiber of the LH figure, it is collimated in the purple beam where the grey modulator controls the transmissions. Either of the 2 fibers on the bottom left can be fed. One or two filter wheels can be integrated to control intensity and/or spectrum width.

9. PERFORMANCE

The Super Stable Source controls an input flux with a variable attenuator in order to reach very high stability. The performance of this system depends mainly on the measurement of the variation and the attenuator dynamics.

The system measuring the flux variations is the photometer, made of the photodetector and the digital multimeter (DMM). The photodetector has a temperature stability of 0.003K over 24 hours with a sensitivity of 5ppm/K, which gives variation amplitudes due to thermal effect below 0.02ppm. The electronic noise of the photodetector at maximal range (10^{10} V/A) is 20 μ V, corresponding to 4ppm for the expected 5V-signal. The DMM reaches 7-digit resolution (0.1ppm) at about 15Hz with a maximum sensitivity of 10 nV and a 24-hour accuracy of 0.6 ppm. Therefore, the measurement uncertainty of the photometer system is about 5ppm at 15Hz and a 24-hour accuracy below 1ppm.

In order to take into account other sources of noise (e.g. antenna effect on cables), the photometer system response to a zero signal has been measured in the configuration of SSS performance tests. The 3-hour response signal had an average value of 245.3 μ V and a standard deviation of 2.5 μ V rms, which corresponds to 0.5ppm for a 5V measurement.

The variations of the LDLS output flux measured by the system in open loop are presented below. This typical result illustrates the specifications of this light source giving a peak-to-peak amplitude of 1.244% and a rms variation of 0.175%. The second graph shows the flux variations between two successive measurements, which correspond to the quantity that has to be balanced by the attenuator in closed loop. Therefore, the maximum common flux variations to be expected are about 2000ppm, which corresponds to a typical attenuator motion of 50 μ m.

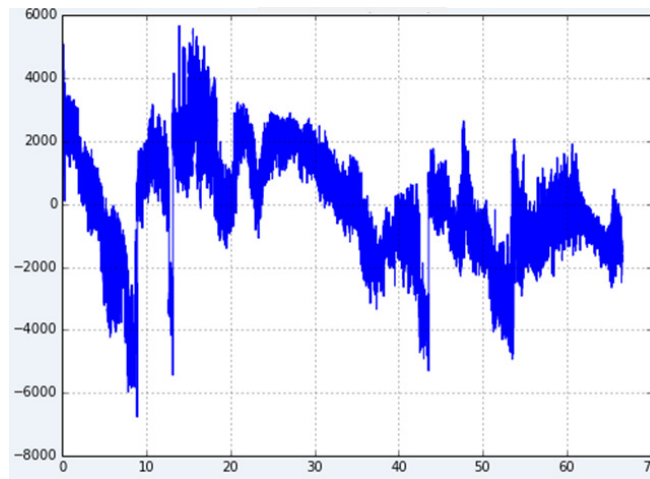


Figure 8. The LDLS flux measured by the photometer systems when the stabilizing loop IS NOT turned on. Note that the vertical axis is given in variations around the mean, expressed in ppm. The horizontal scale is in hours

As described in the previous chapter, the feedback loop has two functioning modes. The first mode (slowest) operates at approximately 8.5Hz for an output signal noise of about 100ppm rms at this frequency, and yields a stability of 4.5ppm when averaged over 60s. The second mode, which we call "continuous", operates at approximately 13.5Hz for an output signal noise of about 85ppm rms, this yields a stability of 3ppm when averaged over 60s. See figures below.

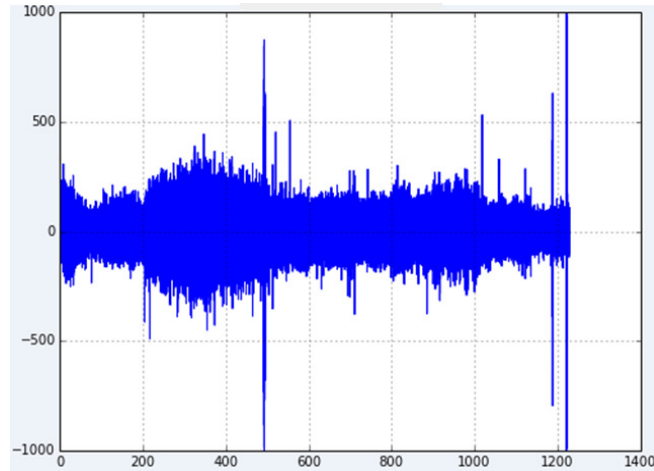


Figure 9. The LDLS flux measured by the photometer systems when the stabilizing loop IS turned on in the continuous mode. Note that the vertical axis is given in variations around the mean, expressed in ppm. The horizontal scale in minutes

CONCLUSION

The system developed to stabilize the optical power of the artificial stars used to test CHEOPS' instrument performance performs exquisitely well. It allows to work with the full bandwidth of the primary source, keep its high radiance while at the same time providing what is arguably the most stable light source in the world

The source stability provided by our system is over a factor of 1000 better than the intrinsic stability of the source, offering a photometric stability in the order of 3ppm for 60s exposures, a typical value for the CHEOPS mission.

REFERENCES

- [1] Benz W. and the Cheops team, CHEOPS: "scientific objectives, mission concept and challenges for the scientific community", the 4S Symposium 2014.
- [2] V. Cessa, T. Beck, W. Benz, C. Broeg, D. Ehrenreich, A. Fortier, G. Peter, D. Magrin, I. Pagano, J.-Y. Plesseria, M. Steller, J. Szoke, N. Thomas, R. Ragazzoni, F. Wildi & the CHEOPS Team. "CHEOPS: A space telescope for ultra-high precision photometry of exoplanet transits", International Conference on Space Optics (ICSO 2014).
- [3] F. Wildi, B. Chazelas, A. Deline, "The On-Ground calibration of the CHEOPS payload", Proc. SPIE 9605-45, (2015)